

UCLA

UCLA Previously Published Works

Title

Tissue Regeneration: A Multifunctional Polymeric Periodontal Membrane with Osteogenic and Antibacterial Characteristics (Adv. Funct. Mater. 3/2018)

Permalink

<https://escholarship.org/uc/item/7hh7d69f>

Journal

Advanced Functional Materials, 28(3)

ISSN

1616-301X

Authors

Nasajpour, Amir
Ansari, Sahar
Rinoldi, Chiara
et al.

Publication Date

2018

DOI

10.1002/adfm.201870021

Peer reviewed

A Multifunctional Polymeric Periodontal Membrane with Osteogenic and Antibacterial Characteristics

Amir Nasajpour, Sahar Ansari, Chiara Rinoldi, Afsaneh Shahrokhi Rad, Tara Aghaloo, Su Ryon Shin, Yogendra Kumar Mishra, Rainer Adelung, Wojciech Swieszkowski, Nasim Annabi, Ali Khademhosseini, Alireza Moshaverinia,* and Ali Tamayol*

Periodontitis is a prevalent chronic, destructive inflammatory disease affecting tooth-supporting tissues in humans. Guided tissue regeneration strategies are widely utilized for periodontal tissue regeneration generally by using a periodontal membrane. The main role of these membranes is to establish a mechanical barrier that prevents the apical migration of the gingival epithelium and hence allowing the growth of periodontal ligament and bone tissue to selectively repopulate the root surface. Currently available membranes have limited bioactivity and regeneration potential. To address such challenges, an osteoconductive, antibacterial, and flexible poly(caprolactone) (PCL) composite membrane containing zinc oxide (ZnO) nanoparticles is developed. The membranes are fabricated through electrospinning of PCL and ZnO particles. The physical properties, mechanical characteristics, and in vitro degradation of the engineered membrane are studied in detail. Also, the osteoconductivity and antibacterial properties of the developed membrane are analyzed in vitro. Moreover, the functionality of the membrane is evaluated with a rat periodontal defect model. The results confirmed that the engineered membrane exerts both osteoconductive and antibacterial properties, demonstrating its great potential for periodontal tissue engineering.

1. Introduction

Periodontitis is a chronic destructive inflammatory disease, which is one of the most prevalent chronic infections in humans.^[1] Periodontal disease leads to the destruction of the periodontium including alveolar bone, the periodontal ligament (PDL), and root cementum.^[1,2] If improperly treated, periodontitis will result in progressive periodontal bone loss that may eventually lead to early tooth loss.^[3] Approximately 35% of the adult human population globally suffers from a moderate form of periodontitis, while a severe generalized form of periodontitis affects around 15% at some stage in their lives. Literature studies have shown that more than 47% of adults aged 30 years and older are diagnosed with some form of periodontal disease.^[4] Furthermore, periodontal disease increases with respect to age. More than 70% of adults aged 65 or older are diagnosed with some form of

A. Nasajpour, C. Rinoldi, Dr. A. S. Rad, Dr. S. R. Shin, Prof. N. Annabi, Prof. A. Khademhosseini, Prof. A. Tamayol
Biomaterials Innovation Research Center
Department of Medicine
Brigham and Women's Hospital
Harvard Medical School
Boston, MA 02139, USA
E-mail: atamayol@bwh.harvard.edu, atamayol@unl.edu

A. Nasajpour, C. Rinoldi, Dr. A. S. Rad, Dr. S. R. Shin, Prof. N. Annabi, Prof. A. Khademhosseini, Prof. A. Tamayol
Harvard-MIT Division of Health Sciences and Technology
Massachusetts Institute of Technology
Cambridge, MA 02139, USA

Dr. S. Ansari, Prof. A. Moshaverinia
Weintraub Center for Reconstructive Biotechnology
Division of Advanced Prosthodontics
School of Dentistry
University of California
Los Angeles, CA 90095-1668, USA
E-mail: a.moshaverinia@ucla.edu

 The ORCID identification number(s) for the author(s) of this article can be found under <https://doi.org/10.1002/adfm.201703437>.

DOI: 10.1002/adfm.201703437

C. Rinoldi, Prof. W. Swieszkowski
Materials Design Division
Faculty of Materials Science and Engineering
Warsaw University of Technology
141 Woloska Str., 02-507 Warsaw, Poland

Prof. T. Aghaloo
Division of Diagnostic and Surgical Sciences
School of Dentistry
University of California
Los Angeles, CA 90095-1668, USA

Dr. S. R. Shin, Prof. N. Annabi, Prof. A. Khademhosseini, Prof. A. Tamayol
Wyss Institute for Biologically Inspired Engineering
Harvard University
Boston, MA 02115, USA

Dr. Y. K. Mishra, Prof. R. Adelung
Functional Nanomaterials Institute for Materials Science
Kiel University
Kaiserstra. 2, D-24143 Kiel, Germany

Prof. N. Annabi
Department of Chemical Engineering
Northeastern University
Boston, MA 02115-5000, USA

periodontal disease. Data from the National Institute of Dental and Craniofacial Research has revealed that nearly 90% of adult populations older than 70 years present at least a moderate level of periodontal-related diseases.^[5] Once damaged, the periodontium has a limited capacity for regeneration. Effective treatment for periodontal disease is of utmost importance, as its consequences can eventually result in tooth loss.

The ultimate goal of periodontal therapy is the regeneration of all the components of the periodontium. Over the past decade, several strategies for periodontal repairing, mainly based on conventional anti-infectious measures, guided tissue regeneration (GTR), or application of cytokines, growth factors, or bioactive molecules, have been followed.^[6] However, the systematic reviews of the clinical outcomes of these procedures show inconsistencies in the results and variable responses.^[7] The significantly high burden of the periodontal disease and its negative consequences on the patient's quality of life indicate a strong need for more effective therapies. Tissue engineering provides a new concept for periodontal tissue regeneration through cell delivery to the damaged sites.^[7] GTR strategies based on the use of periodontal membranes have been suggested for periodontal regeneration.^[8] The periodontal membrane acts as a mechanical barrier which prevents or retards the apical migration of the gingival epithelium and allows periodontal ligament and bone tissue to selectively repopulate the root surface during healing. In addition, GTR membranes should maintain proper properties (e.g., flexibility and degradation profile) that allow for their usage in periodontal defect sites without premature collapsing within the defect site to prevent compromising the regenerative outcome.^[9]

Currently, for GTR procedures both nonabsorbable and absorbable membranes are available.^[5,10] The nonabsorbable membranes require a second surgery for their removal, which can compromise the newly formed tissues. On the other hand, existing biodegradable membranes have a lack of suitable mechanical properties and controlled degradation rate.^[11] Other major drawbacks of the current periodontal membranes are low adhesion to the surrounding tissues, lack of antibacterial properties, and inability to promote tissue regeneration.^[12] For successful periodontal tissue regeneration, adhesion and retention of the membrane to the application site, as well as its regenerative properties, are considered crucial factors. Currently, there is an unmet need for the development of novel biodegradable periodontal membranes, which support adhesion to surrounding tissues, minimize bacterial activity, and induce osteodifferentiation. Electrospun membranes mimic

the microenvironment found within the extracellular matrix and support cellular growth. Electrospun membranes are suturable and typically flexible, the small pore size could effectively prevent the migration of cells across the membrane barrier.^[13] Thus, they could represent an ideal candidate for GTR.

In this study, we have developed and characterized a flexible and biodegradable membrane for treatment of periodontitis via GTR, which could minimize bacterial infection and support osteogenesis. The membranes are electrospun with a dispersed solution of ZnO within a carrier polymer, poly(ϵ -caprolactone) (PCL). The incorporation of ZnO particles not only introduces an antibacterial activity, but also improves the osteoconductivity of the periodontal membrane.^[14] The biological and physical properties of the engineered scaffolds were also assessed. In addition to *in vitro* experiments, we implanted the engineered membrane *in vivo* to assess its functionality within a rat periodontal defect model. The developed membrane provides an appropriate microenvironment to regulate the fate of the local progenitor stem cells toward osteogenic tissues for periodontal tissue regeneration.

2. Results and Discussions

PCL electrospun fibers have proven to be an excellent substrate for bone tissue engineering.^[15] Due to PCL's semi-crystalline nature, the degradation is slow and dependent on the polymer molecular weight.^[16] To render the membranes antibacterial and osteoconductive, we incorporated ZnO particles into the fibrous membranes.^[17] The membranes were fabricated by electrospinning of 10% (w/v) PCL solution in hexafluoroisopropanol containing 0, 0.5, and 1% (w/v) ZnO nanoparticles. The pertinent literature has reported that mixtures carrying less than 2% (w/v) ZnO do not show inhibitory effect on cellular growth, while concentrations above 0.5% (w/v) ZnO can offer antibacterial activity. Thus, we selected the proposed concentrations to assess their effectiveness in osteogenesis.^[18] The nanoparticles were dispersed by sonication and intermittent vortexing. **Figure 1a,b** shows the fabrication process of the membrane and its application for the treatment of periodontium disorders. The morphology of ZnO nanoparticles and the produced fibrous structures are shown in **Figure 1c–e**. The scanning electron microscope (SEM) data suggest that the particles were not monodisperse and their dimensions are in the range of 50–200 nm. The membranes were made of randomly distributed nano/micrometer-sized fibers. The SEM images showed a roughened fiber size after the incorporation of ZnO nanoparticles. The nanoparticle distribution was mapped within the PCL mats using dispersive X-ray microanalysis (energy-dispersive X-ray, EDX) coupled with SEM and the elemental atoms to decipher nanomaterials within the fibrous network. In the membrane composition map, zinc, oxygen, and carbon appeared in the colors aqua, green, and red, respectively (**Figure 1e**; **Figure S1**, Supporting Information). The morphological studies confirmed the uniform distribution of ZnO nanoparticles throughout the fabricated membranes as well as at the surface of the fibers.

The mechanical properties of the engineered membranes were assessed under uniaxial tensile testing and the measured values are reported in stress–strain graphics presented in

Prof. A. Khademhosseini
Center of Nanotechnology
King Abdulaziz University
Jeddah 21569, Saudi Arabia

Prof. A. Khademhosseini
Department of Bioindustrial Technologies
College of Animal Bioscience and Technology
Konkuk University
Seoul, Republic of Korea

Prof. A. Tamayol
Department of Mechanical and Materials Engineering
University of Nebraska, Lincoln
Lincoln, NE 68588, USA

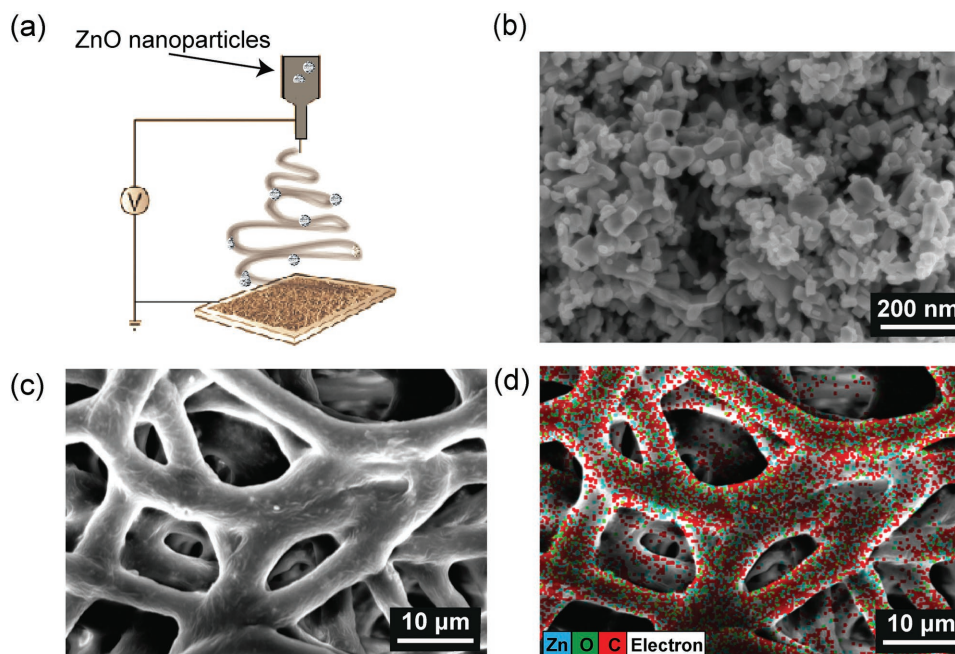


Figure 1. Fabrication of ZnO-doped PCL composite membrane. a) ZnO spherical nanoparticles were embedded within poly(caprolactone) (PCL) and the membrane was fabricated via electrospinning. b) A representative SEM image of ZnO nanoparticles. c) High magnification of membranes containing 1% (w/v) ZnO: the image of the membrane illustrates a rough surface due to incorporation of ZnO nanoparticles. d) EDAX elemental imaging of the membrane with 1% (w/v) ZnO. The aqua colour annotates the atom zinc found in the composite membrane. The image shows a uniform distribution of the spherical particles throughout the membrane.

Figure 2a. The ultimate tensile strength, ultimate strain, and the tensile modulus were calculated from the stress–strain curves. The results suggested that the incorporation of ZnO particles reduced the ultimate strength of the engineered membranes

($p < 0.01$, Figure 2b). The ultimate strain, however, was not significantly changed following ZnO incorporation (Figure 2c). The incorporation of stiff ZnO particles may create cavities within the soft polymer network, but at the same time, higher

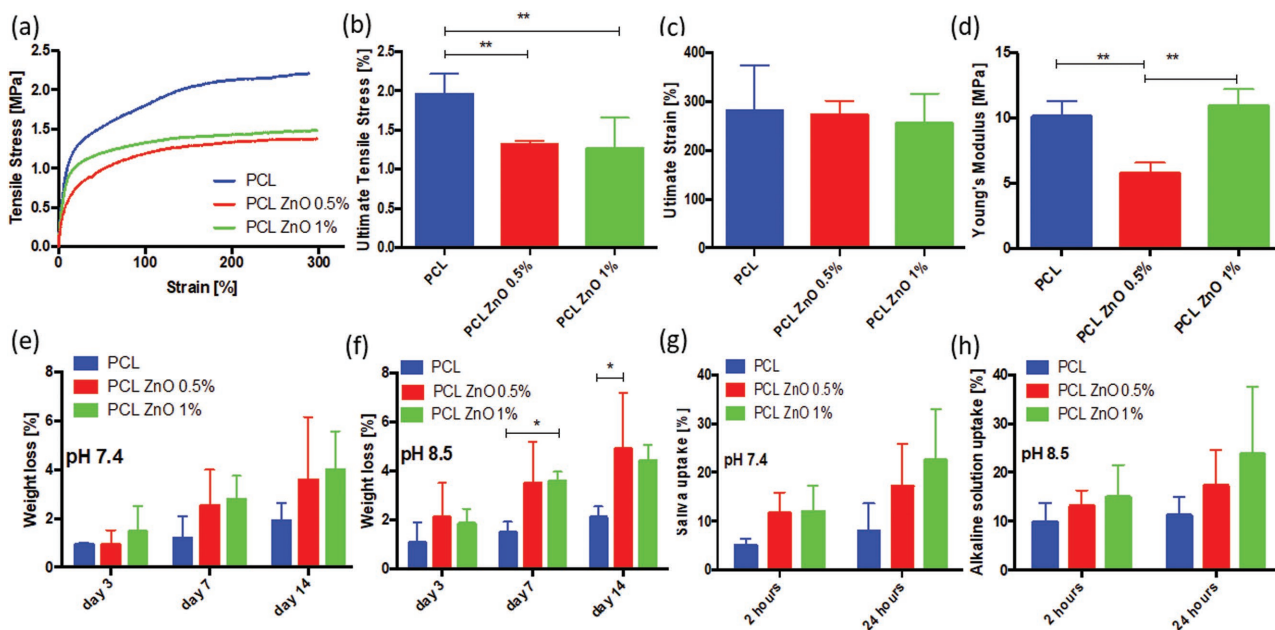


Figure 2. Characterization of engineered membranes containing different amounts of ZnO nanoparticles. a) Representative uniaxial tensile stress–strain curves of electrospun membranes made from pristine PCL, PCL with ZnO 0.5% (w/v), and PCL with ZnO 1% (w/v) solutions. b–d) The mechanical properties obtained from the uniaxial tensile test for the membranes with different ZnO nanoparticle concentration including b) ultimate tensile stress values, c) ultimate strain, and d) Young's Modulus. e, f) Degradation rate of the engineered membranes in e) artificial saliva (pH 7.4) and f) alkaline solution (pH 8.5). g, h) Water uptake of membranes after 2 and 24 h in g) artificial saliva (pH 7.4) and h) phosphate buffer solution (PBS) containing NaOH (pH 8.5). *: $p < 0.05$, **: $p < 0.01$.

concentration of the particles improves the tensile modulus of the composite construct as reported in Figure 2d. This competitive trend has been previously described for composites of polymeric systems doped with dispersed nanoparticles.^[19] Our results suggested that samples containing 0.5% (w/w) of ZnO nanoparticles offered the lowest tensile modulus ($p < 0.01$). Increasing the ZnO nanoparticle concentration enhanced the tensile modulus of membranes to ≈ 10.5 MPa. We also evaluated the degradation of the membranes under two different conditions: soaked in artificial saliva with a pH of 7.4, and in an alkaline environment at pH 8.5. This choice was due to the fact that in a nonhealing wound healing cascade the microenvironment is shifted to a slight alkaline condition. Hence, we tested the degradability of the membranes in a representative alkaline solution. The results suggested that in the presence of ZnO particles, an increase in degradation rate was observed ($p < 0.05$, Figure 2e,f; Figure S2, Supporting Information). This slight increase might be due to the more hydrophilic nature of ZnO, which facilitated the water interaction with the polymeric membranes and its hydrolysis. It should be noted that within 14 d, less than 4% mass loss was observed. The solution uptake was also assessed after 2 and 24 h in both artificial saliva and alkaline solution (pH 8.5). The data suggested a higher uptake in an aqueous solution for membranes containing ZnO nanoparticles (Figure 2g,h; Figure S2, Supporting Information). This result is in agreement with the degradation profiles of the membranes.

We further investigated the function of the engineered periodontal membranes in supporting cellular growth and differentiation. Human periodontal ligament stem cells (PDLSCs) were isolated from periodontal tissues of patients with healthy periodontium as described in the Experimental Section. The cell seeded membranes were incubated in osteogenic

differentiation media for 21 d. Cell proliferation analysis demonstrated that increasing the concentration of ZnO particles from 0 to 1% (w/v) significantly decreased the number of viable cells ($p < 0.05$) in comparison to the pristine PCL membrane or the membrane containing 0.5% (w/v) of ZnO nanoparticles (Figure 3a). This observation could be related to the excessive H_2O_2 production by ZnO nanoparticles, causing high level of reactive oxygen species which was detrimental to cell function.^[20] The alkaline phosphatase (ALP) activity of the seeded cells is presented in Figure 3b. PDLSCs on PCL with 0.5% (w/v) ZnO exhibited the highest ALP activity ($p < 0.05$) at each tested time point. However, no statistically significant difference was observed in ALP activity values between the pristine PCL and the 1% (w/v) ZnO groups. The maximum amount of ALP activity for each group was reported after two weeks of culture.

Since our results described a statistical difference in viability in 1% (w/v) ZnO, we further investigated the potential effect of ZnO incorporated membranes on cellular mediated apoptosis in our tested cultures of PDLSCs. The immunofluorescence staining confirmed an increase expression of apoptotic marker Annexin V in the 1% (w/v) ZnO membrane (Figure 3c,d). However, there was no statistically significant difference between the culture of PDLSCs on pristine PCL and 0.5% (w/v) ZnO membranes.

After two-weeks of osteodifferentiation culture, the results of the Xylenol Orange (XO) staining revealed that PDLSCs seeded on the membrane with 0.5% (w/v) ZnO produced the greatest amounts of mineralized tissue ($p < 0.05$). However, no significant differences were found in the total mineralized tissue as compared to pristine PCL and 1% (w/v) ZnO membranes (Figure 4a,b). Gene expression analysis was also

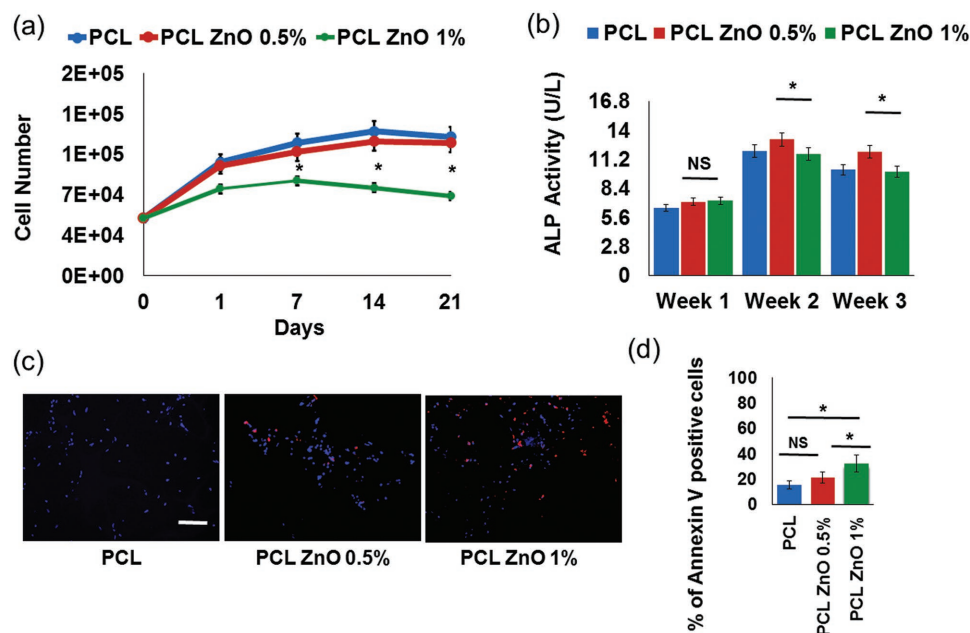


Figure 3. In vitro studies on the engineered membrane. a) Cell proliferation analysis on the surface of PCL engineered membranes containing different concentrations of ZnO nanoparticles. b) Alkaline phosphatase (ALP) activity for PDLSCs seeded on the engineered membranes. The ALP value was normalized to the DNA concentration, with units of ngd-1/ μ g DNA. c,d) Qualitative and quantitative characterization of apoptotic seeded cells. *: $p < 0.05$, NS: not significant. Scale bar represents 200 μ m.

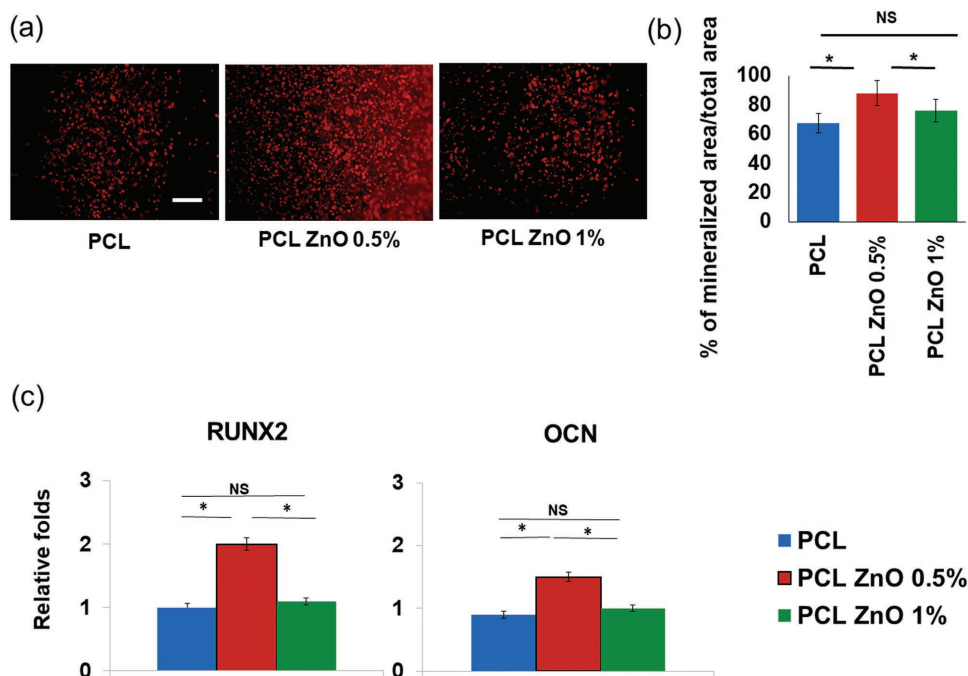


Figure 4. In vitro assessment of osteodifferentiation induced by the engineered membranes. a,b) Qualitative and quantitative measurement of osteodifferentiation of PDLSCs seeded on engineered PCL membranes containing different concentrations of ZnO nanoparticles, using XO staining after two weeks of culture in osteogenic media. Scale bar represents 200 μm . c) Expression level of osteogenic-related genes (Runx2 and OCN) after 2 weeks of osteodifferentiation in vitro evaluated by real time-PCR. Data were normalized by the Ct of the housekeeping gene glyceraldehyde 3-phosphate dehydrogenase (GAPDH) and expressed relatively to gene expression level at day 1 of culture. *: $p < 0.05$; NS: not significant.

performed to evaluate the underlying molecular mechanism of the PDLSCs osteogenic differentiation. Several osteogenic differentiation markers (e.g., Runx2 and osteocalcin (OCN)) were analyzed (Figure 4c). The data confirmed that PDLSCs seeded on 0.5% (w/v) ZnO membranes expressed significantly higher expression levels of Runx2 and OCN after two weeks of in vitro osteogenic induction, in comparison to PDLSCs seeded onto membranes containing 1% (w/v) ZnO.

The antibacterial activity of the engineered membrane was tested against *Porphyromonas gingivalis* ATCC 33277. *P. gingivalis* is a gram negative anaerobic bacterium commonly involved in inducing periodontitis.^[21] We exposed the membranes to different concentrations of bacteria culture and then assessed the number of colony forming units (CFUs) after 1 and 5 d of culture. Obtained data (Figure 5) confirmed the presence of a significant antibacterial activity upon the incorporation of ZnO nanoparticles within the membranes. While pristine PCL failed to exhibit any antibacterial activity after 1 and 5 d of incubation, the membranes containing 0.5% (w/v) and 1% (w/v) of ZnO nanoparticles presented significant antibacterial properties at both time intervals ($p < 0.05$). Based on the promising in vitro experiments on *P. gingivalis* and PDLSCs, it can be concluded that 0.5% (w/v) of ZnO offered some level of antibacterial activity, while supporting the viability and the osteodifferentiation of seeded PDLSCs.

The in vitro data prompted us to evaluate the functionality of the engineered membrane through an animal model. To assess the function of the engineered nanofibrous membrane in healing of periodontal bone defect, we performed a pilot study using a rat periodontal defect model. Our in vitro experiments

suggested a significant difference in the osteoconductivity of the engineered membranes containing ZnO nanoparticles. In addition, since the in vitro data suggested a better cytocompatibility of 0.5% (w/v) ZnO concentration, we only tested the membranes containing this concentration. A periodontal window defect of ≈ 1.5 mm in width, 3 mm in length, and 2 mm in depth was created in lingual of maxillary first molars in 6 rats. Subsequently, the animals were divided into two groups of 3 animals and each group received the following implants at the defect site: (1) sham (negative control) or (2) PCL membrane containing 0.5% ZnO (w/v). The process of implantation is shown in Figure 6a. Animals were sacrificed after 6 weeks and micro-computed tomography (micro-CT) analysis was utilized to examine the amounts of bone regeneration. The vertical bone loss around the defect site was evaluated by measuring the distance between cement-enamel junction (CEJ) and alveolar bone crest at three different points (mesiolingual (ML), mid lingual (L), and distolingual (DL)) on the lingual of the first maxillary molars. Representative micro-CT images before the formation of the defect and 6 weeks after membrane implantation are presented in Figure 6b. All the specimens were standardized and micro-CT images were calibrated for proper comparative analysis. The semi-quantified analysis of the amounts of bone formation at the defect site after 6 weeks showed a smaller distance between the CEJ and the bone crest in the group that was subjected to the implantation of the engineered membrane containing 0.5% (w/v) ZnO nanoparticles. The results proved the effectiveness of the engineered membranes in bone regeneration related to periodontitis. The location of the membrane is not apparent in these images. Further histological analysis is required for detailed

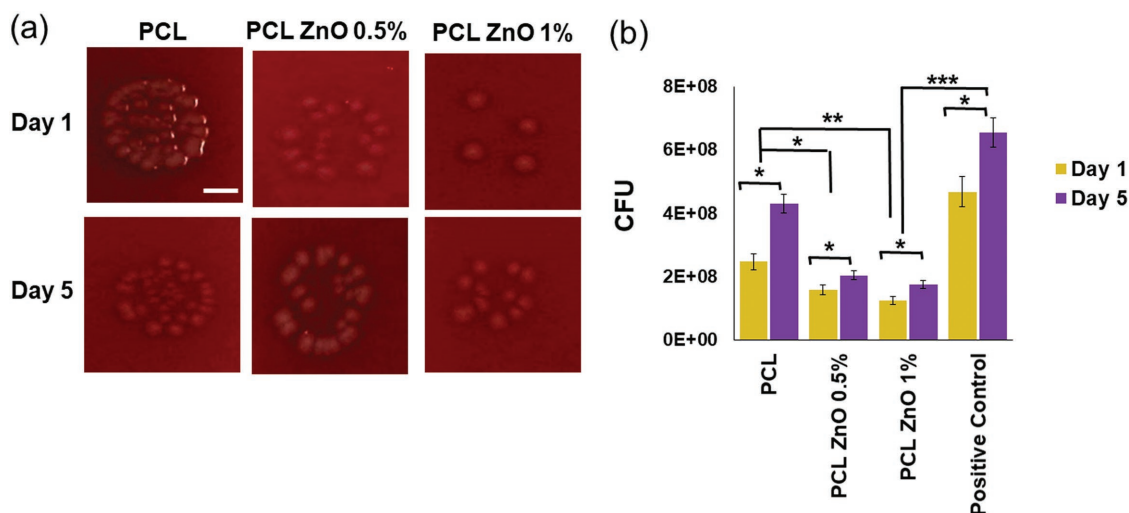


Figure 5. Qualitative and quantitative characterization of the antibacterial properties of PCL engineered membranes containing different concentrations of ZnO nanoparticles. a) Colony forming units (CFUs) of *P. gingivalis* colonies on the surface of the membranes. b) Quantified data on panel (a). *: $p < 0.05$, **: $p < 0.01$, and ***: $p < 0.001$.

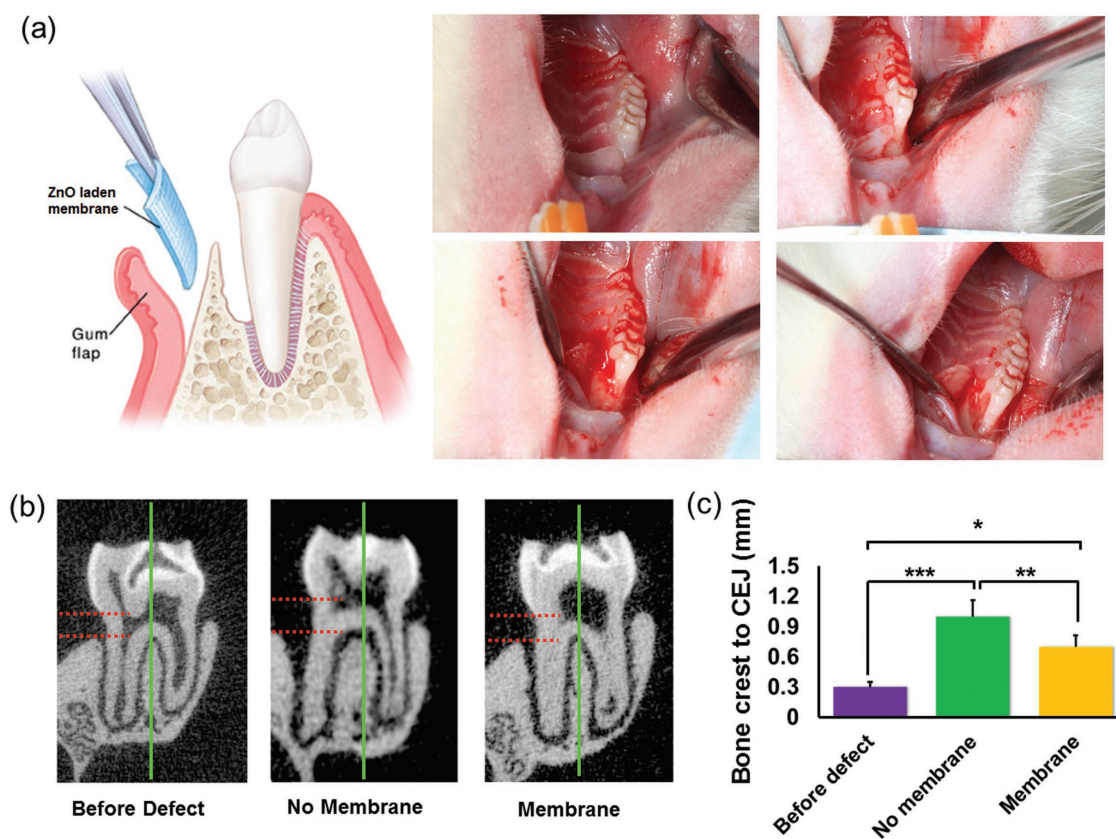


Figure 6. Rat periodontal defect model. a) Depiction of rat periodontal defect design: mucoperiosteal flaps were elevated uncovering the alveolar bone adjacent to the lingual aspect of the first maxillary molar. The alveolar bone covering the root surfaces was removed with a dental bur, creating a periodontal window defect, and the periodontal membrane was placed into the defect site. b) Micro-CT analysis of the rat maxilla showing the control site, the defect site, and the defect size after application of the membrane. All the specimens were standardized and micro-CT images were calibrated for proper comparative analysis. c) Semi-quantitative analysis of the measurements (mm) from CEJ to the bone crest at each time interval (before and after defect, as well as after the membrane application). The transverse plane illustrates the defect and CEJ to bone crest distance. The location of the membrane is not apparent in these images. Further histological analysis is required for detailed evaluation of the amounts of bone regeneration and periodontal repair. * $p < 0.05$, ** $p < 0.01$, *** $p < 0.001$.

evaluation of the amounts of bone regeneration and periodontal repair.

Our *in vitro* data suggest that 0.5% (w/v) ZnO did not show any inhibitory effect on cell activity and function and demonstrated enhanced cell osteodifferentiation in comparison to membranes containing 1% (w/v) ZnO. Our *in vivo* data also support the bone regenerative properties of the developed membranes containing 0.5% (w/v) ZnO via periodontal bone defect model in rats. However, identification of the optimal concentration requires further detailed animal studies. Altogether, our study demonstrated that the developed periodontal membrane is a promising membrane for periodontal regeneration applications *in vitro* and *in vivo*.

3. Conclusions

The goal of this study was to develop a membrane that could be used for treatment of periodontal defects. Altogether, our findings confirmed that we successfully developed a bio-degradable membrane with osteoconductive and antibacterial properties, which can support GTR for the treatment of periodontitis-related bone loss. The fibrous membranes were fabricated via electrospinning of PCL-containing ZnO nanoparticles with tunable mechanical and degradation characteristics. The membranes were flexible, easy to handle, and easy to implant. The results confirmed that incorporation of 0.5% (w/v) ZnO nanoparticles rendered the membranes antibacterial and osteoconductive responses, without negatively impacting their biocompatibility feature. We also demonstrated the *in vivo* functionality of the engineered membrane through a rat periodontal defect model.

4. Experimental Section

Materials: All the chemicals including PCL with $M_n = 80\,000$ and hexafluoroisopropanol were purchased from Sigma-Aldrich (St. Louis, MO) unless mentioned otherwise. The ZnO nanoparticles utilized in the study were provided by Functional Nanomaterials group at Kiel University, Germany.

Fabrication of Nanofibrous Membranes: The PCL-ZnO nanofibrous membranes were fabricated using a conventional electrospinning set-up. Briefly, PCL with $M_n = 80\,000$ was dissolved in hexafluoroisopropanol to achieve a concentration of 10% (w/v). Then ZnO nanoparticles were dispersed in a bath sonicator for 10 min to obtain mixtures containing 0.5 and 1% w/v ZnO particles within the PCL solution. The prepolymer solution was then transferred to a 3 mL syringe with a 20-G blunt needle tip used during the electrospinning process. An electrical field of ≈ 18 kV over a fixed spinning distance of 20 cm was applied. The flow rate of the prepolymer solution was set at 2 mL h^{-1} , and the substrates were spun for 30 min to generate fibrous membranes, which have a thickness of $\approx 100\ \mu\text{m}$. Fibers were collected onto an aluminum flat collector to produce a sheet with uniform fiber distribution.

Optical and Elemental Analysis of Zinc Oxide Composites: The nanocomposite fiber morphology was investigated using a SEM (Zeiss Ultra Plus, 7 kV) with an EDX spectrometer. The nanocomposite fibers were sputtered with gold to reduce the surface charge then compositional analysis was performed in combination with SEM.

Mechanical Characterization of the Engineered Membranes: The mechanical properties of the prepared scaffolds were measured using a uniaxial tensile strength test with a universal mechanical testing

machine (Instron 5542, Norwood, MA). Five samples of each membrane were tailored in rectangular-shaped ($20\text{ mm} \times 5\text{ mm}$), positioned between two grips and subjected on tensile displacement. The constant crosshead speed was set at 10 mm min^{-1} and the related force was measured using a 10 N cell. The modulus of elasticity was calculated using the initial 0–10% linear region of the stress–strain curves for five samples and the mean values \pm standard deviations were reported.

Swelling and Degradation Analysis: Fluid handling capacity was performed by soaking the dry membranes ($1\text{ cm} \times 1\text{ cm}$) in 2 mL of NaOH based-solution (basic pH = 8.5) and separately in 2 mL of saliva mimicking solution containing 0.4 g L^{-1} KCl, 0.4 g L^{-1} NaCl, 0.906 g L^{-1} $\text{CaCl}_2 \cdot 2\text{H}_2\text{O}$, 0.690 g L^{-1} $\text{NaH}_2\text{PO}_4 \cdot 2\text{H}_2\text{O}$, 0.005 g L^{-1} $\text{Na}_2\text{S}_2\text{O}_8 \cdot \text{H}_2\text{O}$, and 1 g L^{-1} urea.^[22] The weight before and after 2 and 24 h of immersion in the solutions were measured with a high precision scale to assess the swelling ratio.

The degradation rate of the membranes was evaluated by placing square samples measuring $1\text{ cm} \times 1\text{ cm}$ in 2 mL solution of artificial saliva (neutral pH = 7.5), and NaOH based-alkaline solution (basic pH = 8.5). The specimen weight was measured before the experiment and then after 1, 3, 7, and 14 d using a high precision scale.

In Vitro Assessment of Osteoconductivity of Membranes Containing ZnO Particles—Progenitor Cell Isolation and Culture: Teeth and PDL tissues were obtained from healthy male patients (18–25 years old) undergoing third molar extractions according to IRB approval. Subjects with a history of periodontal disease were excluded from this study. Human PDLSCs were isolated and cultured according to published protocols in the literature.^[23]

Cell Seeding and Proliferation Analysis: All the fabricated disk-shaped membranes (PCL, PCL with 0.5% (w/v) ZnO or PCL with 1% (w/v) ZnO) were prewetted and sterilized in 70% ethanol for 2 h, washed with PBS, and soaked in a serum free culture medium overnight before cell seeding. PDLSCs were seeded onto the membranes at a density of 5×10^4 cells cm^{-2} and cultured in culture medium containing alpha-MEM with 15% FBS, $2 \times 10^{-3}\text{ M}$ L-glutamine, $100 \times 10^{-9}\text{ M}$ Dex, $100 \times 10^{-6}\text{ M}$ ascorbic acid, 100 U mL^{-1} penicillin, and $100\ \mu\text{g mL}^{-1}$ streptomycin (Sigma, St. Louis, MO) for three weeks.

At different time intervals (1, 7, 14, and 21 d) the number of living cells was analyzed using Alamar Blue assay (ThermoFischer). ALP activity was also determined based on previously published protocols.^[24] Additionally, after two weeks of culture, apoptosis of the seeded MSCs was analyzed using FACSCalibur (BD Bioscience) flow cytometry by staining the cells with Annexin V-PE Apoptosis Detection Kit I (BD Bioscience). Additionally, the specimens were immunofluorescently stained using antibodies against Annexin V.

In Vitro Osteogenic Differentiation of PDLSCs: PDLSCs were seeded onto different fabricated membranes and cultured for two weeks. To induce osteogenesis, the specimens were placed in an osteogenic medium containing alpha-MEM, 10% FBS, 1% penicillin, streptomycin, and dexamethasone ($0.1 \times 10^{-3}\text{ M}$), beta-glycerophosphate ($10 \times 10^{-3}\text{ M}$), $1.8 \times 10^{-3}\text{ M}$ potassium dihydrogen phosphate, and ascorbic acid (50 mg mL^{-1}).

After 2 weeks of culture in osteogenic differentiation medium, the samples were stained with Xylenol Orange (XO). The expression levels of Runx2 and ALP (Santa Cruz Biosciences, Dallas, TX) were assayed by PCR analysis.

In Vitro Assessment of Antibacterial Activity of Membranes Containing ZnO Particles: To evaluate the antibacterial activity and properties of the engineered membranes, PCL, PCL with 0.5% ZnO, and PCL with 1% ZnO were tested against *P. gingivalis* (P.g.). *P. gingivalis* ATCC 33277 was grown anaerobically (80% N_2 , 10% CO_2 , 10% H_2) in Columbia Broth (CB) with hemin ($5\ \mu\text{g mL}^{-1}$) and menadione ($1\ \mu\text{g mL}^{-1}$) as supplements for 15–18 h. The culture was further adjusted to an optical density of 0.1 to be used in coinoculation with the membrane samples.

Membranes were sectioned into 8 mm diameter discs with a biopsy punch in aseptic conditions. Five discs of each membrane type were tailored. The membrane discs were inoculated in 48 wells plate in 1 mL 0.1 OD of *P. gingivalis* ATCC 33277 in CB with hemin ($5\ \mu\text{g mL}^{-1}$) and menadione ($1\ \mu\text{g mL}^{-1}$). One disc with CB alone served as negative

control. For the positive control, 0.1 OD of *P. gingivalis* was grown without the disc.

Subsequently, a direct inhibition of bacterial growth onto the membranes was performed by counting CFU after incubation for 1 and 5 d at 37 °C in an anaerobic chamber. Aliquots of culture medium were then taken from each well, serially diluted, and placed on agar plates. The viability of *P. gingivalis* was analyzed on CB blood agar plates with hemin (5 µg mL⁻¹) and menadione (1 µg mL⁻¹) by spotting 20 µL of the serially diluted samples in CB (10¹ to 10⁷). The colonies were counted after incubation of the plates in an anaerobic chamber for 3–5 d.

In Vivo Assessment of the Membrane Function: A rat periodontal defect model (Figure 6) was considered. Ten, two-month-old virgin male and female Spraguee Dawley rats (Harlan Laboratories, Livermore, CA) were utilized for testing the ZnO membrane in vivo. The test was performed according to approved protocols. Briefly, mucoperiosteal flaps were elevated uncovering the alveolar bone adjacent to the lingual aspect of the first maxillary molars. The alveolar bone covering the root surfaces on the lingual side was removed with a dental bur under saline irrigation. A periodontal window defect of ≈1.5 mm in width, 3 mm in length, and 2 mm in depth was created. Subsequently, one of the following membranes was implanted into the defect site: (1) Sham, (2) PCL membrane, or (3) PCL membrane with 0.5% ZnO. Animals were sacrificed after 6 weeks and micro-CT analysis was used to examine the amounts of bone regeneration. The vertical bone loss around the defect site was evaluated by measuring the distance between CEJ and alveolar bone crest at three different points (mesiolingual (ML), mid lingual (L), and distolingual (DL)) on the lingual of the first maxillary molars.

Statistical Analysis: All measurements were made at least in triplicate, and data were presented as mean values ± standard deviation. One-way Anova test was performed and differences were considered statistically significant when *p* values resulted lower than 0.05: **p* < 0.05, ***p* < 0.01, ****p* < 0.001.

Supporting Information

Supporting Information is available from the Wiley Online Library or from the author.

Acknowledgements

A.N. and S.A. contributed equally to this work. This work was supported by ONR PECEASE Award, and the National Institutes of Health (Grant Nos. HL092836, DE019024, EB012597, AR057837, DE021468, HL099073, EB008392, and DE023825). C.R. would like to thank the funding from the National Centre for Research and Development in the frame of START project (STRATEGMED1/233224/10/NCBR/2014). Y.K.M. and R.A. acknowledge the financial support from Deutsche Forschungsgemeinschaft (DFG) under schemes AD/183/10-1, AD 183/17-1, and under GRK 2154, Project P3. A.N. would like to acknowledge Dr. Anas Chalah (Harvard University) for inspiration during class discussion. A.T. acknowledges the financial support from Startup Fund provided by the University of Nebraska-Lincoln.

Conflict of Interest

The authors declare no conflict of interest.

Keywords

electrospinning, guided tissue regeneration, osteoconductive, periodontal regeneration, zinc oxide

Received: June 23, 2017

Revised: July 25, 2017

Published online: November 10, 2017

- [1] B. L. Pihlstrom, B. S. Michalowicz, N. W. Johnson, *Lancet* **2005**, 366, 1809.
- [2] G. Polimeni, A. V. Xiropaidis, U. M. Wikesjo, *Periodontology* **2000** **2006**, 41, 30.
- [3] a) F. M. Chen, J. Zhang, M. Zhang, Y. An, F. Chen, Z. F. Wu, *Biomaterials* **2010**, 31, 7892; b) E. Alsberg, K. W. Anderson, A. Albeiruti, R. T. Franceschi, D. J. Mooney, *J. Dent. Res.* **2001**, 80, 2025.
- [4] A. Amano, J. Murakami, S. Akiyama, I. Morisaki, *Jpn. Dent. Sci. Rev.* **2008**, 44, 118.
- [5] L. J. Jin, G. C. Armitage, B. Klinge, N. P. Lang, M. Tonetti, R. C. Williams, *Adv. Dent. Res.* **2011**, 23, 221.
- [6] M. C. Bottino, V. Thomas, *Front. Oral Biol.* **2015**, 17, 90.
- [7] M. C. Bottino, V. Thomas, G. Schmidt, Y. K. Vohra, T. M. Chu, M. J. Kowolik, G. M. Janowski, *Dent. Mater.* **2012**, 28, 703.
- [8] a) L. Larsson, A. M. Decker, L. Nibali, S. P. Piliplchuk, T. Berglundh, W. V. Giannobile, *J. Dent. Res.* **2015**, 95, 255; b) K. H. Kim, L. Jeong, H. N. Park, S. Y. Shin, W. H. Park, S. C. Lee, T. I. Kim, Y. J. Park, Y. J. Seol, Y. M. Lee, Y. Ku, I. C. Rhyu, S. B. Han, C. P. Chung, *J. Biotechnol.* **2015**, 120, 327; c) R. E. Jung, G. A. Halg, D. S. Thoma, C. H. Hammerle, *Clin. Oral Implants Res.* **2009**, 20, 162.
- [9] E. A. Munchow, M. T. Albuquerque, B. Zero, K. Kamocki, E. Piva, R. L. Gregory, M. C. Bottino, *Dent. Mater.* **2015**, 31, 1038.
- [10] a) Y. D. Rakhmatia, Y. Ayukawa, A. Furuhashi, K. Koyano, *J. Prosthodontics Res.* **2013**, 57, 3; b) S. Y. Shin, H. N. Park, K. H. Kim, M. H. Lee, Y. S. Choi, Y. J. Park, Y. M. Lee, Y. Ku, I. C. Rhyu, S. B. Han, S. J. Lee, C. P. Chung, *J. Periodontol.* **2005**, 76, 1778; c) M. Kikuchi, Y. Koyama, T. Yamada, Y. Imamura, T. Okada, N. Shirahama, K. Akita, K. Takakuda, J. Tanaka, *Biomaterials* **2004**, 25, 5979.
- [11] R. E. Jung, N. Fenner, C. H. F. Hämmerle, N. U. Zitzmann, *Clin. Oral Implants Res.* **2013**, 24, 1065.
- [12] J. Behring, R. Junker, X. F. Walboomers, B. Chessnut, J. A. Jansen, *Odontology* **2008**, 96, 1.
- [13] a) W. J. Li, C. T. Laurencin, E. J. Caterson, R. S. Tuan, F. K. Ko, *J. Biomed. Mater. Res., Part A* **2002**, 60, 613; b) M. C. Bottino, V. Thomas, G. Schmidt, Y. K. Vohra, T.-M. G. Chu, M. J. Kowolik, G. M. Janowski, *Dent. Mater.* **2012**, 28, 703; c) A. H. Najafabadi, A. Tamayol, N. Annabi, M. Ochoa, P. Mostafalu, M. Akbari, M. Nikkhal, R. Rahimi, M. R. Dokmeci, S. Sonkusale, B. Ziaie, A. Khademhosseini, *Adv. Mater.* **2014**, 26, 5823.
- [14] a) K. T. Shalumon, K. H. Anulekha, S. V. Nair, S. V. Nair, K. P. Chennazhi, R. Jayakumar, *Int. J. Biol. Macromol.* **2011**, 49, 247; b) P. Feng, P. Wei, C. Shuai, S. Peng, *PLoS One* **2014**, 9, e87755.
- [15] H. Yoshimoto, Y. M. Shin, H. Terai, J. P. Vacanti, *Biomaterials* **2003**, 24, 2077.
- [16] H. Sun, L. Mei, C. Song, X. Cui, P. Wang, *Biomaterials* **2006**, 27, 1735.
- [17] a) R. Augustine, N. Kalarikkal, S. Thomas, *Int. J. Polym. Mater. Polym. Biomater.* **2016**, 65, 28; b) H. Papavlassopoulos, Y. K. Mishra, S. Kaps, I. Paulowicz, R. Abdelaziz, M. Elbahri, E. Maser, R. Adelung, C. Röhl, *PLoS One* **2014**, 9, e84983.
- [18] R. Augustine, H. N. Malik, D. K. Singhal, A. Mukherjee, D. Malakar, N. Kalarikkal, S. Thomas, *J. Polym. Res.* **2014**, 21, 347.
- [19] S. N. Raja, A. J. Luong, W. Zhang, L. Lin, R. O. Ritchie, A. P. Alivisatos, *Chem. Mater.* **2016**, 28, 2540.
- [20] P. Kocbek, K. Teskač, M. E. Kreft, J. Kristl, *Small* **2010**, 6, 1908.
- [21] K. J. Baek, S. Ji, Y. C. Kim, Y. Choi, *Virulence* **2015**, 6, 274.
- [22] T. Fusayama, T. Katayori, S. Nomoto, *J. Dent. Res.* **1963**, 42, 1183.
- [23] A. Moshaverinia, C. Chen, X. Xu, K. Akiyama, S. Ansari, H. H. Zadeh, S. Shi, *Tissue Eng., Part A* **2014**, 20, 611.
- [24] V. M. C. Quent, D. Loessner, T. Friis, J. C. Reichert, D. W. Hutmacher, *J. Cell. Mol. Med.* **2010**, 14, 1003.